

# Electron-energy-loss functions of the solid fullerenes C<sub>60</sub> and C<sub>70</sub>

V. I. Rubtsov and Yu. M. Shul'ga

*Institute of Chemical Physics, Russian Academy of Sciences, Chernogolovka, 142432, Moscow Oblast*  
(Submitted 20 October 1992)

Zh. Eksp. Teor. Fiz. **103**, 2065–2071 (June 1993)

Electron-energy-loss spectra of the individual fullerenes C<sub>60</sub> and C<sub>70</sub> have been measured at primary-electron energies from 250 to 2000 eV in a reflection geometry. After the background due to multiple scattering of electrons is subtracted, the loss functions of the fullerenes, averaged over scattering angle, are obtained. The  $\pi$ -plasmon peak is more intense for C<sub>70</sub> than for C<sub>60</sub>. The primary distinction between the loss spectra of the fullerenes and those of graphite-like materials is that the region between the plasmon peaks is more intense in the case of the fullerenes.

Electron-energy-loss spectroscopy (EELS) has been used quite extensively to study the electronic structure of fullerenes.<sup>1–11</sup> The first results found, during the passage of electrons with energies of 50–200 keV through thin layers of the test material,<sup>1–3</sup> were quite different from the results found by other methods, e.g., through study of the spectral fine structure near the C1s photoelectron peak<sup>4–6</sup> or through study<sup>7,8</sup> of the spectrum of reflected electrons with energies of 75–200 eV. Differences stemming from a component of the measured spectrum due to either losses within a carbon atom with a vacancy in the 1s level (in the case of the photoelectron spectra) or multiple-scattering losses (in the reflected-electron spectra) distorted the spectrum. The peak corresponding to the  $\sigma + \pi$  plasmon was effectively shifted to a higher loss. Incorporating the multiple-scattering loss in the case of the reflected-electron spectra cures this problem and provides a solid foundation for identifying the corrected spectrum with the loss function.<sup>12</sup>

Our purposes in the present study were to measure EELS spectra for the individual fullerenes C<sub>60</sub> and C<sub>70</sub> in a reflection geometry for various energies of the primary beam (250–2000 eV), to subtract from these spectra the background due to multiple-scattering losses, to distinguish the fullerene loss function  $\text{Im}(-1/\epsilon)$  ( $\epsilon$  is the dielectric constant), and to compare the resulting loss functions with each other and with those for graphite.

The fullerenes C<sub>60</sub> (with a purity of better than 99.9%) and C<sub>70</sub> (99.7%), in the form of black polycrystalline powders, were prepared by the method described previously.<sup>9,10</sup> Fullerene samples for the spectroscopy were prepared by depositing the fullerenes on an aluminum substrate. The substrate was first cleaned and then oxidized in air to form a thin oxide film, with a thickness of 20–40 Å. It was assumed that this film would prevent a possible chemical interaction between the fullerenes and the substrate. The thickness of the fullerene coating in the analysis zone was 0.2–0.7  $\mu\text{m}$ .

The EELS spectra were measured on a PHI-551 spectrometer equipped with a double-cylindrical-mirror analyzer, with an attachment for angular measurements and with an electron gun coaxial with the analyzer. The analyzer was operated in a retarding-potential mode (the en-

ergy of the electrons passing through the analyzer was 25 eV) at an absolute resolution of 0.7 eV. The energy of the primary electrons ( $E_p$ ) was varied from 250 to 2000 eV. The half-width of the energy distribution of the primary beam was 0.5 eV. The samples were positioned in such a way that the angle of incidence of the primary electrons ( $\alpha$ ) was equal to the angle at which the reflected electrons were detected ( $\beta$ ). Under the condition  $\alpha = \beta$ , we used two different positions for the samples:  $\alpha = 70^\circ$  ("normal" incidence) and  $\alpha = 10^\circ$  ("grazing" incidence with respect to the surface of the sample). The angular resolution was  $8^\circ$ . The residual gas pressure in the spectrometer chamber was no greater than  $3 \cdot 10^{-10}$  torr.

The resulting spectra were corrected for the kinetic-energy dependence of the transmission coefficient of the analyzer. The single-scattering loss spectra  $y(E)$  were found by solving the integral equation<sup>12</sup>

$$N^{\text{in}}(E) - ky(E) * N^{\text{in}}(E) = ky(E), \quad (1)$$

where the asterisk (\*) means an energy convolution,  $N^{\text{in}}(E)$  is the inelastic part of the measured EELS spectrum, normalized to the area under the elastic peak, and the factor  $k$  reflects the geometry of the electron-reflection experiment.

The function  $y(E)$  found in this manner is proportional to the loss function averaged over scattering angle:<sup>12</sup>

$$y(E) \sim \ln(1 + \theta_{\text{max}}^2 / \theta_E^2) \text{Im}(1/\epsilon(E)), \quad (2)$$

where  $\theta_{\text{max}}$  is the maximum angle of scattering by valence electrons, and we have  $\theta_E = E/(2E_p)$ . For brevity we call  $y(E)$  the "loss function." One advantage of our approach is that it does not require any special assumptions regarding the specific energy dependence of the differential cross section for inelastic scattering for the plasmon channel and other electron-scattering channels. Figure 1 illustrates the sequence of operations carried out to find the function  $y(E)$  from the experimental spectrum.

Figure 2 shows loss functions  $y(E)$  for all the samples studied. All the spectra have two primary peaks, which, by analogy with graphite, are attributed to the excitation of plasma oscillations of all the valence electrons (a  $\sigma + \pi$  plasmon) and to the excitation of  $\pi$  electrons alone (a  $\pi$  plasmon). Table I shows the positions of the  $y(E)$  peaks

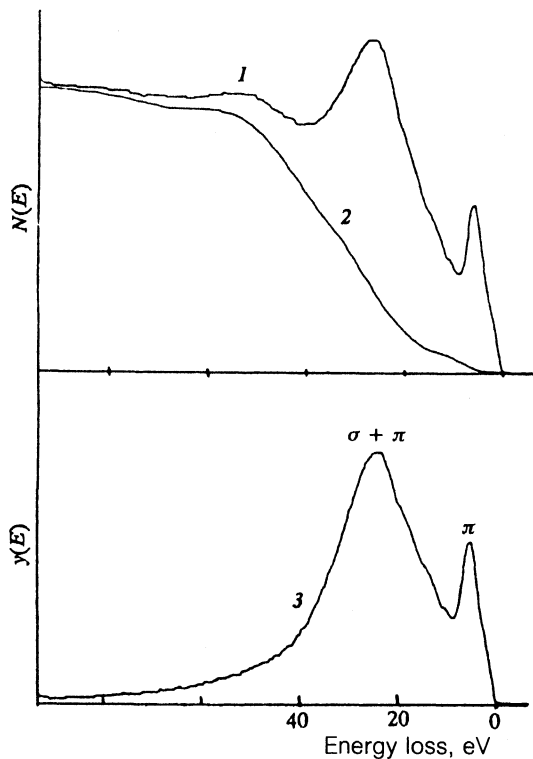


FIG. 1. 1—Experimental electron-energy-loss spectrum for  $C_{60}$  before the subtraction of the background; 2—the background of multiply scattered electrons; 3—the loss function.  $E_p=2$  keV.

for the test samples. When the background of multiple-scattering losses is subtracted, the peak corresponding to the  $\sigma+\pi$  plasmon shifts 1–2 eV toward a lower electron energy loss. We see from Table I that the switch from a normal observation angle to a grazing one leads to no systematic shift of the peaks in the loss function for the fullerenes, while an angular dependence is observed in the case of graphite. The energy positions of the  $\sigma+\pi$  peak for  $C_{70}$  are approximately the same as those for  $C_{60}$  over the range of primary-electron energies used.

For graphite single crystals, the positions of the peaks in the loss spectrum depend on the angle between the electron momentum and the  $c$  axis of the crystal. For the polycrystalline graphite samples, this dependence is averaged out, and the value  $\hbar\omega_{\sigma+\pi}=26\text{--}27$  eV is found.<sup>13</sup> Fink *et al.*<sup>14</sup> have reported a value of 24.5 eV for the energy of the  $\sigma+\pi$  plasmon for amorphous carbon. For less dense  $a\text{-C:H}$  samples, the energy of the  $\sigma+\pi$  plasmon is in the interval 20.8–24.0 eV, depending on the conditions under which the samples are prepared.<sup>14,15</sup> For graphite-like materials there is a correlation: With increasing mass density  $\rho$  of the material in the analysis zone in the EELS measurements, the energy of the main plasmon increases.<sup>15</sup> This correlation indicates that polycrystalline fullerenes should lie between polycrystalline graphite (2.25 g/cm<sup>3</sup>) and amorphous carbon (1.9 g/cm<sup>3</sup>) in terms of the value of  $\rho$ . However, the value of the density for a solid  $C_{60}$  is<sup>16</sup>  $\rho=1.65$  g/cm<sup>3</sup>. The energy of the main plasmon for

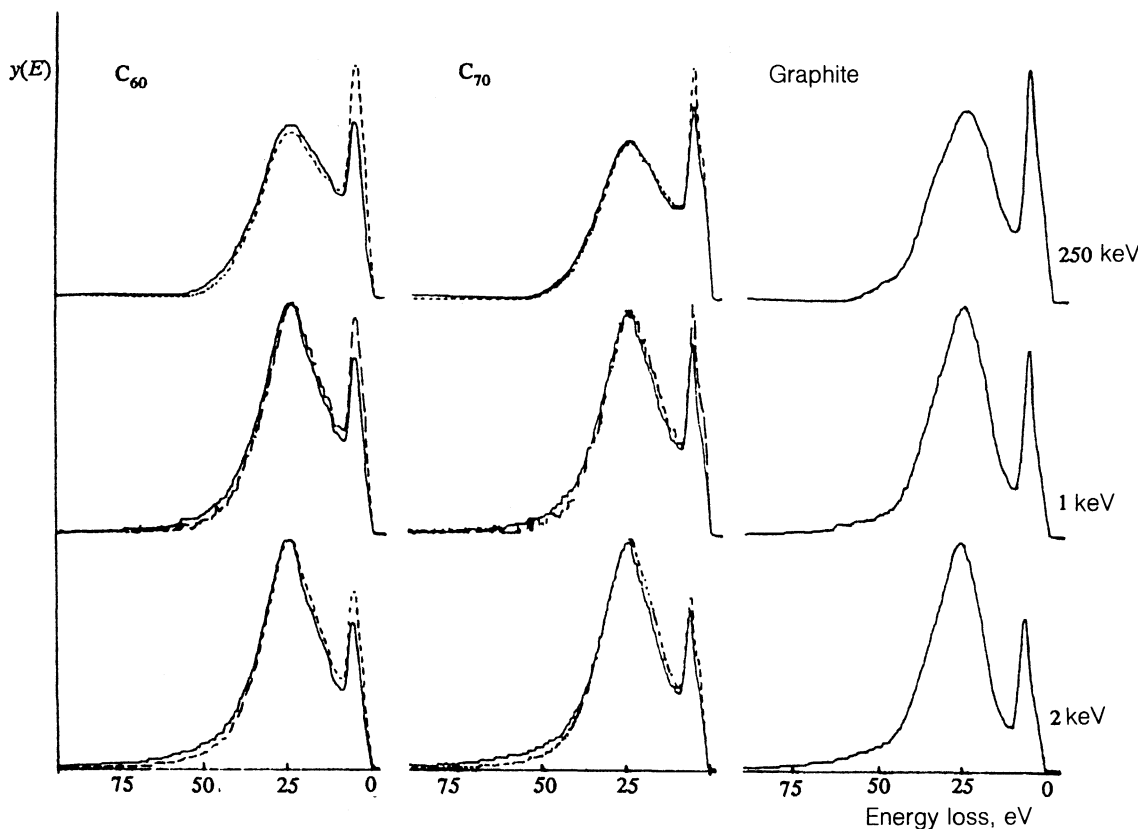


FIG. 2. The function  $y(E)$  for  $C_{60}$  (at the left), for  $C_{70}$  (in the middle), and for graphite (at the right) for primary beam energies of 250 eV (top), 1 keV (middle), and 2 keV (bottom). Solid lines—"Normal" incidence; broken line—"grazing" incidence.

TABLE I. Positions (in eV) of the peaks in the function  $y(E)$  for  $\alpha=70^\circ$ .

Sample	Peak	Energy of primary electrons		
		250 eV	1 keV	2 keV
C <sub>60</sub>	$\sigma + \pi$	25,0(24,6)	24,8(25,0)	25,0(24,4)
	$\pi$	5,8(5,6)	5,8(5,6)	5,8(5,6)
C <sub>70</sub>	$\sigma + \pi$	25,1(25,0)	24,8(24,3)	24,8(24,0)
	$\pi$	5,6(5,6)	5,8(5,6)	5,6(5,6)
Graphite	$\sigma + \pi$	25,5(18,6)	26,2	26,4
	$\pi$	6,4(6,5)	6,4	6,4

Note: Data for the “grazing” angle of incidence are shown in parentheses.

fullerene-based materials thus does not reflect the average density over the volume. This conclusion agrees with the conclusions of Refs. 2 and 9.

The primary difference between the single-scattering-loss spectra of the fullerenes and graphite is that in the case of the fullerenes the intensity is higher in the region between the main peaks. In terms of energy position, there may be losses here due to transitions from the part of the valence band between “pure”  $\pi$  states (the upper part of the valence band) and “pure”  $\sigma$  states (the lower part) to one of the unfilled subbands above the Fermi level. Just why the probability for these transitions is higher in the fullerenes than in graphite-like materials is not clear at this point. In a recent theoretical derivation of the electromagnetic response of C<sub>60</sub>, it was also noted that there is a wide band of transitions at “intermediate” energies,<sup>17</sup>  $\hbar\omega=10-20$  eV. A comparative analysis, however, will require corresponding calculations for clusters modeling graphite. We might add that the large half-width of the  $\sigma + \pi$  peak of the fullerenes in comparison with that of graphite may be a consequence of the higher intensity between the main peaks.

It can also be seen from Fig. 2 that the relative intensity of the  $\pi$  plasmon increases with decreasing energy of the primary electrons,  $E_p$ . The relative intensity of the  $\pi$ -plasmon peak was found from

$$I_\pi = \left\{ \int_0^{E_{\min}} y(E) dE \right\} / \left\{ \int_0^{E_{\max}} y(E) dE \right\}, \quad (3)$$

where  $E_{\min}$  is the energy corresponding to the position of the local minimum in the function  $y(E)$  between the main peaks, and  $E_{\max}$  is the maximum measured value of the loss energy ( $E_{\max}=95$  eV in the case at hand). Figure 3 shows the relative intensity  $I_\pi$  as a function of the energy of the primary electrons. The decrease in  $I_\pi$  with increasing energy of the primary beam can be attributed to a change in the probability for the excitation of the  $\pi$  plasmon. We might add that the relative intensity of the  $\pi$ -plasmon peak at a primary energy  $E_p=100$  keV is only 1–2% for the fullerenes (this is our estimate based on a figure in Ref. 3).

It can also be seen from Fig. 3 that for  $\alpha=70^\circ$  the relation  $I_\pi(C_{70}) > I_\pi(C_{60})$  holds. The same effect was observed in Ref. 3, although the difference was less obvious

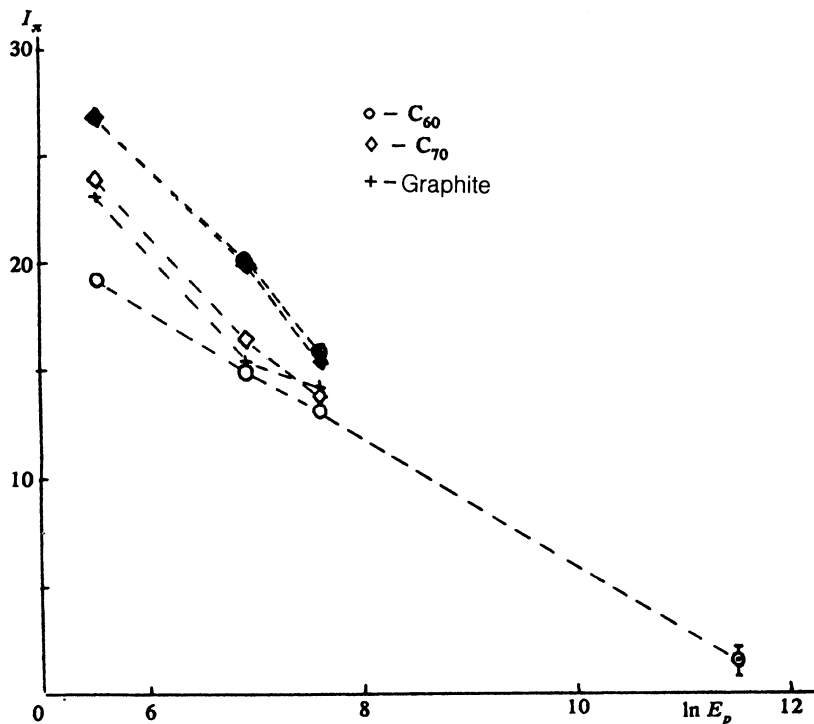


FIG. 3. Relative intensity  $I_\pi$  (see the text proper) as a function of  $\ln E_p$ . The point with error bars at the lower right was extracted from a figure in Ref. 3. The filled symbols show data for a “grazing” detection angle.

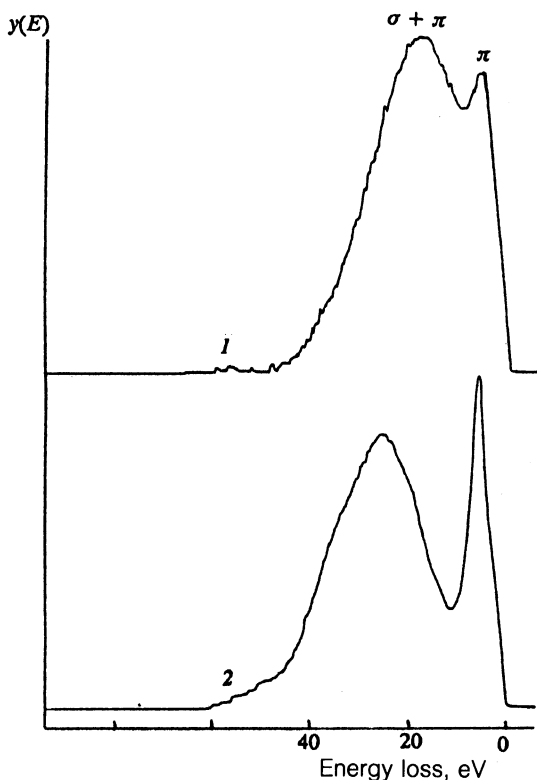


FIG. 4. The function  $y(E)$  for graphite for detection angles of  $70^\circ$  (1) and  $10^\circ$  (2).  $E_p = 250$  eV.

there. As we go from  $\alpha = 70^\circ$  to  $\alpha = 10^\circ$ , the relative intensity of the  $\pi$ -plasmon peak increases for both fullerenes, while the difference between  $I_\pi(C_{60})$  and  $I_\pi(C_{70})$  essentially vanishes.

For graphite the value of  $I_\pi$  at the detection angle of  $70^\circ$  with respect to the surface of the sample lies between the values of  $I_\pi$  for  $C_{60}$  and  $C_{70}$ . At the grazing angle, the shape of the function  $y(E)$  for graphite changes sharply (Fig. 4). The peak corresponding to the  $\sigma + \pi$  plasmon shifts to a lower energy, and the relative intensity of the  $\pi$  peak decreases. The apparent reason is that surface defects (steps, curled ends of interrupted planes, etc.) dominate the spectrum for graphite at the grazing angle. The density of valence electrons is typically lower for these defects, and the relative number of  $\pi$  electrons smaller. Caputi *et al.*,<sup>18</sup> studied the dependence of the shape of the loss spectrum

on the detection angle; their results agree with those of the present study.

In summary, the single-scattering loss spectra of the fullerenes  $C_{60}$  and  $C_{70}$ , like those of graphite-like materials, have two main peaks, one due to the excitation of a  $\sigma + \pi$  plasmon and the other due to the excitation of a  $\pi$  plasmon. In terms of the energy of the  $\sigma + \pi$  plasmon, the fullerenes occupy an intermediate position between graphite and amorphous (or glassy) carbon. The relative intensity of the  $\pi$ -plasmon peak is higher for  $C_{70}$  than for  $C_{60}$ . The primary distinction between the loss spectra of the fullerenes and those of graphite-like materials is that the intensity is higher in the region between the main peaks in the case of the fullerenes.

We wish to thank A. S. Lobach and A. P. Moravskii for furnishing the characterized fullerene powders and for a useful discussion.

- <sup>1</sup>Y. Saito, H. Shinohara, and A. Ohshita, *Jpn. J. Appl. Phys.* **30**, L1068 (1991).
- <sup>2</sup>P. L. Hansen, P. J. Fallon, and W. Fratschmer, *Chem. Phys. Lett.* **181**, 367 (1991).
- <sup>3</sup>V. P. Dravid, S. Lin, and M. M. Kappes, *Chem. Phys. Lett.* **185**, 75 (1991).
- <sup>4</sup>J. H. Weaver, J. L. Martin, T. Komeda *et al.*, *Phys. Rev. Lett.* **66**, 1741 (1991).
- <sup>5</sup>M. B. Jost, N. Troullier, D. M. Poirier *et al.*, *Phys. Rev. B* **44**, 1966 (1991).
- <sup>6</sup>P. J. Benning, D. M. Poirier, T. R. Ohno *et al.*, *Phys. Rev. B* **44**, 1962 (1991).
- <sup>7</sup>W. M. Tong, D. A. A. Olberg, H. K. You *et al.*, *J. Chem. Phys.* **95**, 4709 (1991).
- <sup>8</sup>G. Gensterblum, J. J. Pireaux, P. A. Thiry *et al.*, *Phys. Rev. Lett.* **67**, 2171 (1991).
- <sup>9</sup>Yu. M. Shul'ga, A. P. Moravskii, A. S. Lobach, and V. I. Rybtsov, *Pis'ma Zh. Eksp. Teor. Fiz.* **55**, 137 (1992) [*JETP Lett.* **55**, 132 (1992)].
- <sup>10</sup>Yu. M. Shul'ga, V. I. Rubtsov, A. P. Moravskii, and A. S. Lobach, *Dokl. Akad. Nauk SSSR* **325**, 779 (1992).
- <sup>11</sup>E. Solmen, J. Fink, and W. Kratschmer, *Z. Phys. B* **86**, 87 (1992).
- <sup>12</sup>G. M. Mikhaïlov and V. I. Rubtsov, *Poverkhnost'*, No. 7, 99 (1987).
- <sup>13</sup>H.-C. Tsai and D. B. Bodi, *J. Vac. Sci. Technol. A* **5**, 3287 (1987).
- <sup>14</sup>J. Fink, T. Muller-Heinzerling, J. Pfluger *et al.*, *Solid State Commun.* **47**, 687 (1983).
- <sup>15</sup>I. Muhling, K. Bewilogua, and K. Brener, *Thin Solid Films* **187**, 65 (1990).
- <sup>16</sup>W. Kratschmer, L. D. Lamb, K. Fostiropoulos, and D. R. Huffman, *Nature* **347**, 354 (1990).
- <sup>17</sup>G. F. Bertsch, A. Bulgac, D. Tomanek, and Y. Wang, *Phys. Rev. Lett.* **67**, 2690 (1991).
- <sup>18</sup>L. S. Caputi, G. Chiarello, A. Santaniello *et al.*, *Phys. Rev. B* **34**, 6080 (1986).

Translated by D. Parsons